A LETTERS JOURNAL EXPLORING THE FRONTIERS OF PHYSICS

Società Italiana di Fisica

sciences IOP Institute of Physics

LETTER

$ZnIr_2O_4$: An efficient photocatalyst with Rashba splitting

To cite this article: Nirpendra Singh and Udo Schwingenschlögl 2013 *EPL* **104** 37002

View the article online for updates and enhancements.

You may also like

- Silicene/ZnI_2 van der Waals heterostructure: tunable structural and electronic properties
Md. Sakib Hassan, Md. Sherajul Islam and Jeongwon Park
- DFT study of the electronic and optical properties of ternary chalcogenides AlX_2Te_4
Sikander Azam, Muhammad Irfan, Zeesham Abbas et al.
- Construction of noble-metal-free TiO_2 nanobelt/$ZnIn_2S_4$ nanosheet heterojunction nanocomposite for highly efficient photocatalytic hydrogen evolution
Na Wei, Yanhao Wu, Mingliang Wang et al.

This content was downloaded from IP address 18.116.80.213 on 25/04/2024 at 23:24

A Letters Journal Exploring the Frontiers of Physics

November 2013

EPL, **104** (2013) 37002
doi: 10.1209/0295-5075/104/37002

www.epljournal.org

$ZnIr_2O_4$: An efficient photocatalyst with Rashba splitting

Nirpendra Singh[a] and Udo Schwingenschlögl[b]

Physical Science & Engineering Division, KAUST - Thuwal 23955–6900, Kingdom of Saudi Arabia

received 11 July 2013; accepted in final form 4 November 2013
published online 29 November 2013

PACS 71.20.-b – Electron density of states and band structure of crystalline solids
PACS 78.20.-e – Optical properties of bulk materials and thin films

Abstract – Semiconductor-based photocatalysts nowadays are of central interest for the splitting of water into hydrogen and oxygen. However, the efficiency of the known materials is small for direct utilization of the solar energy. Using first-principles calculations, we show that $ZnIr_2O_4$ can overcome this shortage. Modified Becke-Johnson calculations give an indirect band of 2.25 eV, which can be reduced to the visible energy range by S doping. For 25% S doping we find a direct band gap of 1.25 eV and a Rashba spin splitting of 220 meVÅ. The valence band edge potential is 2.89 V against the standard hydrogen electrode, which is sufficient for photocatalytic water oxidation and pollutant degradation. The optical absorption of S-doped $ZnIr_2O_4$ is strongly enhanced, making the material an efficient photocatalyst for visible light.

Copyright © EPLA, 2013

Introduction. – The photocatalytic production of H_2 and O_2 by water splitting using oxide semiconductors receives increasing interest in view of a more efficient utilization of solar energy [1,2]. Oxide-semiconductor–based photocatalysts are suitable for water splitting and the decomposition of organic pollutants [3–6], where the photocatalytic reaction is governed by the absorption of photons, the separation and migration of the generated charges (electron-hole pairs) and the redox reaction on the surface of the material. Upon excitation of electrons from the valence band (VB) into the conduction band (CB) by light with an energy above the band gap of the semiconductor, the separated electrons and holes can move to the surface of the material and react with water [7], where some of them will recombine before the reaction. In general, the redox ability of a semiconductor is related to the positions of the VB and CB edges. When the CB edge potential is more negative than the H potential and the VB edge potential is more positive than the O potential, it is (theoretically) possible to decompose water into H_2 and O_2 without electric power [1]. A proper band gap therefore is of primary importance for the photocatalytic reaction. On the other hand, factors such as carrier transport, surface states, and chemical stability also must be taken into account for an efficient photocatalytic decomposition of water.

Among the oxide semiconductors, TiO_2 shows a strong redox potential as well as a high activity. However, its band gap (3.2 eV) is so wide that it absorbs only ultraviolet light and thus utilizes only 3% to 5% of the solar energy. Specific requirements for a high quantum efficiency therefore are 1) a band gap below 2 eV, 2) a negative potential of the CB edge relative to the H^+/H_2 potential, and 3) stability in aqueous solution after the light irradiation. The H^+/H_2 potential is located 4.5 eV below the vacuum level. In metal oxides a band gap can arise not only between the O $2p$ VB and metal CB but also within the metal bands, for example when the transition metal ions experience an octahedral crystal field and the t_{2g} states are filled with six electrons. For transition metal $3d$ states the band gap is usually much smaller than the 1.5 to 2 eV needed for direct photoelectrochemical H_2 production. However, larger band gaps may be obtained in compounds with stronger hybridization with the ligands, especially in $4d$ and $5d$ oxides. Among the $4d$ oxides, the electronic structure and optical properties of spinel $ZnRh_2O_4$ are well studied and a band gap of 1.2 eV is reported [8]. The ability of this compound to serve as a solar H_2 photocatalyst has been investigated in ref. [9] and the analogous $5d$ spinel oxide $ZnIr_2O_4$ has been reported to be a p-type semiconductor [10]. In this context, we present *ab initio* calculations of the electronic structure and optical properties of $ZnIr_2O_4$ and S-doped $ZnIr_2O_4$, with an eye on photoelectrochemical applications.

Methods. – Within density functional theory the local density approximation (LDA) and generalized gradient approximation (GGA) are used most commonly for treating

[a]E-mail: nirpendra.singh@kaust.edu.sa
[b]E-mail: udo.schwingenschlogl@kaust.edu.sa

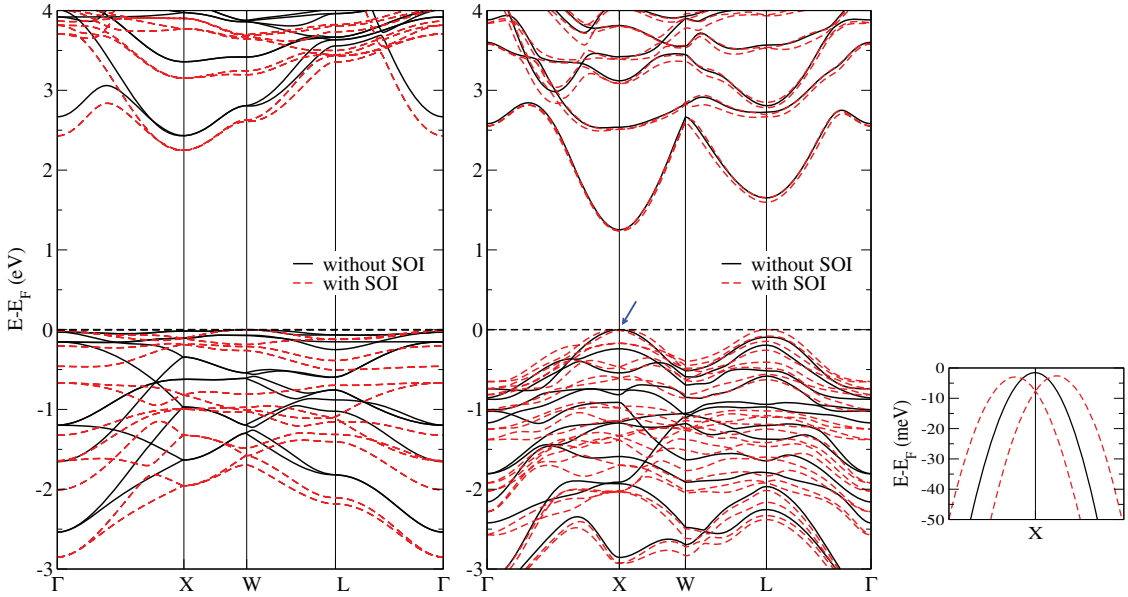

Fig. 1: (Colour on-line) Electronic band structure of $ZnIr_2O_4$ and S-doped $ZnIr_2O_4$. On the right-hand side a zoom of the region around the X point (see arrow) is shown.

the exchange correlation potential. However, these methods underestimate semiconductor band gaps. A feasible way to improve the calculated band gaps is the modified Becke-Johnson (mBJ) exchange potential [11]. Being computationally economical as the LDA/GGA and avoiding atom-dependent parameters, the mBJ exchange plus LDA correlation (mBJLDA) potential yields an orbitally independent, semi-local exchange correlation potential that has proven to result in accurate band gaps for wide-gap insulators, *sp* semiconductors, and 3*d* transition metal oxides [12]. In ref. [13] this approach has been successfully applied to calculate the photocatalytic properties of a MoS_2 monolayer. We will consequently employ the mBJLDA potential in the following and compare the results to the GGA (in the Perdew-Burke-Ernzerhof flavor) using the full potential linearized augmented plane-wave approach implemented in WIEN2k [14], which has proven accuracy in many instances to describe the electronic structure, optical spectrum, and catalytic properties of materials [15–17].

We model 25% of S doping by replacing one O atom with S in the $ZnIr_2O_4$ unit cell. We start from the experimental lattice parameter (8.503 Å) and atomic coordinates [10] and fully optimize the crystal structure by minimizing the atomic forces. We use a **k**-mesh of $12 \times 12 \times 12$ points for the band structure and density of states (DOS) and a dense **k**-mesh of $18 \times 18 \times 18$ points for the optical calculations. The spin orbit interaction (SOI) is incorporated via the second variational method [18]. The product $R_{mt}K_{max}$, where K_{max} is the maximum length of all **k**-vectors and R_{mt} is the smallest muffin-tin radius, controls the size of the basis set and is set to a high value of 7, with a cutoff of the charge-density Fourier expansion of 12. The following muffin-tin radii are employed: 2.1 bohr for Zn/Ir and 1.6 bohr for O/S. Beyond, a maximum value of $\ell_{max} = 12$ is used in the expansion of the basis functions inside the atomic spheres. The dielectric function $\varepsilon(\omega) = \varepsilon_1(\omega) + i\varepsilon_2(\omega)$ describes the optical response [19,20], where the imaginary part is calculated by summing all transitions from occupied to unoccupied states over the Brillouin zone, weighted with the transition probabilities. The real part then is obtained by the Kramers-Kronig relation. The optical absorption is calculated as $\alpha(\omega) = \sqrt{2}\omega\sqrt{|\varepsilon(\omega)| - \varepsilon_1(\omega)}$.

Results and discussion. – The electronic band structures of $ZnIr_2O_4$ and S-doped $ZnIr_2O_4$ obtained by the mBJLDA approach with and without SOI are shown in fig. 1. The VB maximum (represented by a dashed line) appears at the X high-symmetry point, while the CB minimum is observed at the W point. As a consequence, $ZnIr_2O_4$ is an indirect band gap semiconductor (2.25 eV between X and W) with a direct gap of 2.35 eV at the X point. Without SOI the band gap is larger (2.45 eV) consistent with calculations using the HSE06 hybrid functional [21]. In the latter calculations the authors have not considered the SOI, which is essential because of the Ir. For the GGA the indirect band gap is strongly underestimated with a value of 0.61 eV. As compared to the VB edge the bands at the CB edge are more dispersive, which indicates that the photogenerated electrons possess a small effective mass and thus a high ability of migration. The band structure of S-doped $ZnIr_2O_4$ shows a direct band gap of 1.25 eV at the X high-symmetry point and, by close inspection, a Rashba splitting (see the zoom shown in fig. 1) due to the combination of the strong SOI of

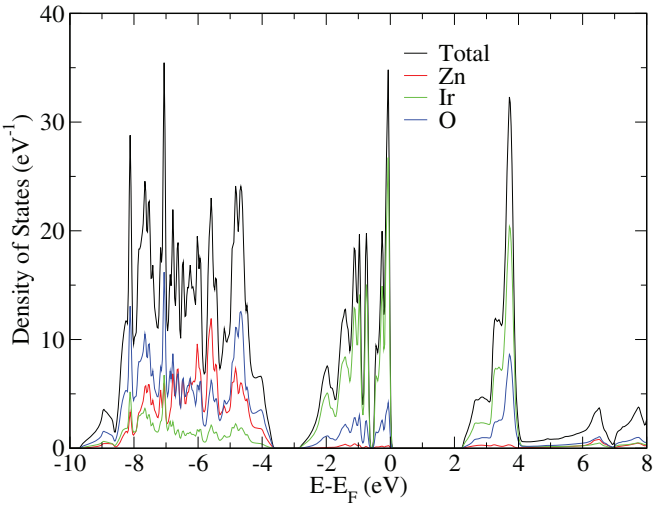

Fig. 2: (Colour on-line) Total and partial densities of states of $ZnIr_2O_4$.

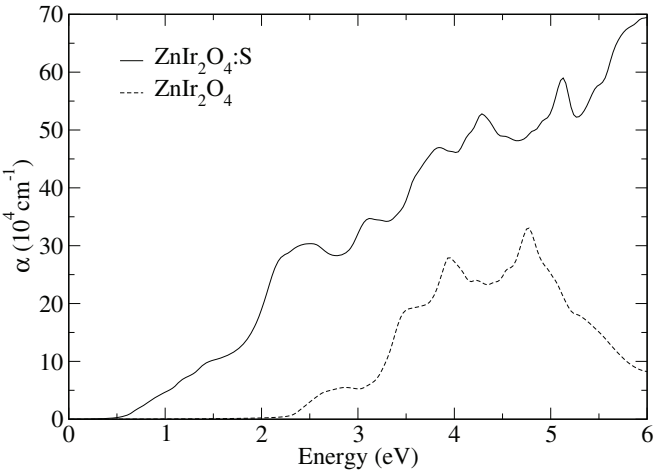

Fig. 3: Absorption spectra of $ZnIr_2O_4$ and S-doped $ZnIr_2O_4$.

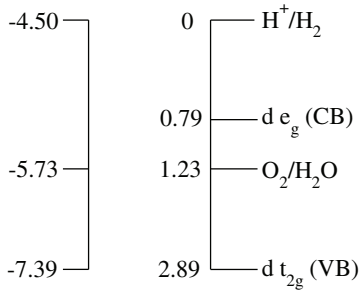

Fig. 4: Energy diagram with the VB and CB edge potentials of $ZnIr_2O_4$.

Ir and the broken inversion symmetry by S doping. Never before a Rashba splitting has been reported for a doped spinel compound. The characteristic parameters quantifying the strength of the splitting are the Rashba energy E_R and the coupling constant $\alpha_R = 2E_R/k_R$ [22,23], where k_R is the momentum offset. We obtain $E_R = 4.5\,\text{meV}$ and $k_R = 44\,\text{Å}^{-1}$, which results in a substantial Rashba parameter of $\alpha_R = 220\,\text{meVÅ}$.

The DOS of $ZnIr_2O_4$ consists of several manifolds, see fig. 2, which are, in the order of increasing energy: 1) O $2p$ derived bands from $-9\,\text{eV}$ to $-4\,\text{eV}$, 2) Ir t_{2g} derived bands from $-3\,\text{eV}$ to the VB maximum, 3) Ir e_g derived bands from the CB minimum to 6 eV, and 4) Zn s and p derived bands from 6 eV to 8 eV. Figure 2 shows that both the Ir t_{2g} and e_g manifolds are narrow as is typical for the localized states of spinel transition metal oxides. According to our results, the band gap is located between the crystal-field split Ir $4d$ manifolds, while the O $2p$ states appear at lower energy. The basic scenario described above for potential oxide photoelectrode materials therefore is realized in $ZnIr_2O_4$. The DOS of S-doped $ZnIr_2O_4$ exhibits the same characteristic features as found for pristine $ZnIr_2O_4$.

In general, optical spectra involve matrix elements, which are crucial in the present case due to the d-d character of the dominating transition (forbidden by dipole selection rules). As a consequence, the hybridization with the ligands and the dispersion are key quantities. The calculated absorption spectrum of $ZnIr_2O_4$ in fig. 3 is in agreement with the experiment [10]. The $\sim 3\,\text{eV}$ absorption peak has a significant value of $5 \cdot 10^4\,\text{cm}^{-1}$. For a S doping of 25% in $ZnIr_2O_4$ the absorption is enhanced by a factor of approximately six to a value of $30 \cdot 10^4\,\text{cm}^{-1}$ at 2.5 eV. This high value demonstrates that S-doped $ZnIr_2O_4$ is an excellent photocatalyst for visible light.

The redox ability of a compound can be estimated by determining the energetic positions of the VB and CB edges using the Mulliken electronegativity [24]: $E_{VB} = \chi_{sc} - E_e + 0.5E_g$ and $E_{CB} = E_{VB} - E_g$, where E_{VB} and E_{CB} are the VB edge and CB edge potentials, χ_{sc} is the electronegativity of the semiconductor (the geometric mean of the electronegativities of the constituent atoms), $E_e = 4.5\,\text{eV}$ is the standard electrode potential on the hydrogen scale, and E_g is the band gap as obtained from the mBJLDA calculation. For $ZnIr_2O_4$ we obtain an electronegativity of 6.34 eV. Figure 4 summarizes the calculated edge potentials: The VB edge potential is 2.89 V, *i.e.*, higher than that of O_2/H_2O (1.23 V). Therefore, $ZnIr_2O_4$ has the ability to oxidize H_2O to produce O_2 or oxidation pollutants. In contrast, the CB edge potential is 0.79 V, *i.e.*, higher than that of H^+/H_2 (0 V), such that $ZnIr_2O_4$ cannot reduce H^+ to H_2. By S doping the VB edge potential shifts down to 2.30 V but is still high enough for the reduction of H^+ to H_2 due to the high CB edge potential. Because of the higher absorption in the visible region, S doping increases the efficiency of H_2O oxidation to produce O_2. We note that besides the band alignment for practical purposes the surface properties of a material are of equal importance [25–27]. Concerning the exposed metal cations that can be active sites, it can be expected that $ZnIr_2O_4$ resembles the behavior of the isostructural compound $ZnGa_2O_4$ as reported in ref. [28].

Conclusion. – To conclude, the band structure, density of states, and optical spectrum of $ZnIr_2O_4$ and S-doped $ZnIr_2O_4$ have been calculated using the GGA and mBJLDA approaches with and without SOI. The mBJLDA band gap is 2.25 eV with SOI and, consequently, a good approximation of the experimental band gap. It turns out that the band gap appears between the crystal-field split Ir $5d$ states, with t_{2g} VB and e_g CB. The mBJLDA approach leads to a VB edge potential of 2.89 V against the standard hydrogen electrode and a CB edge potential of 0.79 V. Therefore, $ZnIr_2O_4$ has the ability to oxidize H_2O but cannot reduce H^+. S doping reduces the band gap and thus induces a significant optical absorption in the visible light range. This fact strongly improves the efficiency of the electrochemical decomposition. In addition, we have demonstrated that S doping leads to a Rashba splitting of the electronic bands at the X point with a magnitude of 220 meV Å, which constitutes the first case that Rashba splitting is found in a doped spinel compound.

REFERENCES

[1] Fujishima A. and Honda K., *Nature*, **238** (1972) 37.
[2] Asahi R., Morikawa T., Ohwaki T., Aoki K. and Taga Y., *Science*, **293** (2001) 269.
[3] Zou Z., Ye J., Sayama K. and Arakawa H., *Nature*, **414** (2001) 625.
[4] Chen X., Shen S., Guo L. and Mao S. S., *Chem. Rev.*, **110** (2010) 6503.
[5] Tachikawa T., Fujitsuka M. and Majima T., *J. Phys. Chem. C*, **111** (2007) 5259.
[6] Minggu L. J., Wan Daud W. R. and Kassim M. B., *Int. J. Hydrogen Energy*, **35** (2010) 5233.
[7] Linsebigler A. L., Lu G. and Yates J. T. jr., *Chem. Rev.*, **95** (1995) 735.
[8] Singh D. J., Rai R. C., Musfeldt J. L., Auluck S., Singh N., Khalifah P., McClure S. and Mandrus D. G., *Chem. Mater.*, **18** (2006) 2696.
[9] Takimotoa Y., Kittaa T. and Irie H., *Int. J. Hydrogen Energy*, **37** (2012) 134.
[10] Dekkers M., Rijnders G. and Blank D. H. A., *Appl. Phys. Lett.*, **90** (2007) 021903.
[11] Tran F. and Blaha P., *Phys. Rev. Lett.*, **102** (2009) 226401.
[12] Singh D. J., *Phys. Rev. B*, **82** (2010) 205102.
[13] Singh N., Jabbour G. and Schwingenschlögl U., *Eur. Phys. J. B*, **85** (2012) 392.
[14] Blaha P., Schwarz K ., Madsen G. K. H., Kvasnicka D. and Luitz J., *WIEN2k, An Augmented Plane Wave+ Local Orbitals Program for Calculating Crystal Properties* (TU Vienna, Vienna) 2001.
[15] Singh N., Saini S. M., Nautiyal T. and Auluck S., *J. Appl. Phys.*, **100** (2006) 083525.
[16] Singh N. and Schwingenschlögl U., *Appl. Phys. Lett.*, **100** (2012) 151906.
[17] Sayede A., Khenata R., Chahed A. and Benhelal O., *J. Appl. Phys.*, **113** (2013) 173501.
[18] Koelling D. D. and Harmon B. N., *J. Phys. C*, **10** (1977) 3107.
[19] Wooten F., *Optical Properties of Solids* (Academic Press, New York) 1972.
[20] Yu Y. P. and Cardona M., *Fundamentals of Semiconductors: Physics and Materials Properties* (Springer, Berlin) 1999.
[21] Scanlon D. O. and Watson G. W., *Phys. Chem. Chem. Phys.*, **13** (2011) 9667.
[22] Ast C. R., Henk J., Ernst A., Moreschini L., Falub M. C., Pacile D., Bruno P., Kern K. and Grioni M., *Phys. Rev. Lett.*, **98** (2007) 186807.
[23] Martin C., Mun E. D., Berger H., Zapf V. S. and Tanner D. B., *Phys. Rev. B*, **87** (2013) 041104(R).
[24] Nethercot A. H., *Phys. Rev. Lett.*, **33** (1974) 1088.
[25] Li Y.-F., Liu Z.-P. and Gao W., *J. Am. Chem. Soc.*, **132** (2010) 13008.
[26] Li Y.-F. and Liu Z.-P., *J. Am. Chem. Soc.*, **133** (2011) 15743.
[27] Li Y.-F. and Liu Z.-P., *Phys. Chem. Chem. Phys.*, **15** (2013) 1082.
[28] Jia C., Fan W., Yang F., Zhao X., Sun H., Li P. and Liu L., *Langmuir*, **29** (2013) 7025.